Repeatable Generalized Inverse Control Strategies for Kinematically Redundant Manipulators

Rodney G. Roberts and Anthony A. Maciejewski

Abstract—**Kinematically redundant manipulators possess an infinite number of joint angle trajectories which satisfy a given desired end effector trajectory. The joint angle trajectories considered in this work are locally described by generalized inverses which satisfy the Jacobian equation relating the instantaneous joint angle velocities to the velocity of the end effector. One typically selects a solution from this set based on the local optimization of some desired physical property such as the minimization of the norm of the joint angle velocities, kinetic energy, etc. Unfortunately, this type of solution frequently does not possess the desirable property of repeatability in the sense that closed trajectories in the workspace are not necessarily mapped to closed trajectories in the joint space. In this work, the issue of generating a repeatable control strategy which possesses the desirable physical properties of a particular generalized inverse is addressed. The technique described is fully general and only requires a knowledge of the associated null space of the desired inverse. While an analytical representation of the null vector is desirable, ultimately the calculations are done numerically so that a numerical knowledge of the associated null vector is sufficient. This method first characterizes repeatable strategies using a set of orthonormal basis functions to describe the null space of these transformations. The optimal repeatable inverse is then obtained by projecting the null space of the desired generalized inverse onto each of these basis functions. The resulting inverse is guaranteed to be the closest repeatable inverse to the desired inverse, in an integral norm sense, from the set of all inverses spanned by the selected basis functions. This technique is illustrated for a planar, three degree-of-freedom manipulator and a seven degree-of-freedom spatial manipulator.**

I. INTRODUCTION

A robotic manipulator is described by its kinematic equation which relates the joint configuration of the manipulator to the position and orientation of the end effector in the workspace. The kinematic equation f: $\Theta \rightarrow \mathscr{W}$ is usually a nonlinear mapping of the manipulator's joint space Θ to the workspace $\mathscr{W}$ where $\dim(\Theta) = n$ and $\dim(\mathscr{W}) = m$. More specifically, this equation is given by

$$x = f(\theta) \tag{1}$$

Manuscript received February 27, 1991; revised January 16, 1992 and August 19, 1992. Paper recommended by Associate Editor, K. Furuta.

This work was supported by Sandia National Laboratories under Grant 18-4379B. Additional support was provided by the NEC Corporation and the TRW Foundation.

The authors are with the School of Electrical Engineering, Purdue University, West Lafayette, IN 47907.

IEEE Log Number 9208450.

where x is an m-vector and θ is an n-vector. One of the popular techniques for controlling a manipulator is resolved motion rate control [20] which calculates the joint velocities from the joint configuration and desired end effector velocity. The underlying equation is the Jacobian equation which, for the positional components, can be found by differentiating (1) to obtain

$$\dot{x} = J\dot{\theta} \tag{2}$$

where $\dot{x}$ is the desired end effector velocity. The chief advantage of using the Jacobian for the motion control of a manipulator is that the Jacobian is a linear relationship between the joint velocities and the end effector velocities. At each point θ, J is an $m \times n$ matrix.

Kinematically redundant manipulators are robotic systems which possess more degrees of freedom than are required for a specified task. This occurs when $m < n$. This additional freedom offers obvious advantages over conventional nonredundant manipulators including the potential for obstacle avoidance, torque minimization, singularity avoidance, and greater dexterity [1], [3], [5], [7], [8], [11], [14], [21]–[23]. There are an infinite number of control strategies for redundant manipulators. One can take advantage of this freedom by choosing a control strategy which will optimize some particular criterion. A popular optimal control strategy is the minimum norm solution

$$\dot{\theta} = J^{+}\dot{x} \tag{3}$$

where J^{+} is the Moore–Penrose pseudoinverse of J. This control strategy locally minimizes the joint velocities of the manipulator subject to moving the end effector along a specified trajectory. Equation (3) can be generalized to include all solutions by adding terms in the null space of J resulting in

$$\dot{\theta} = J^{+}\dot{x} + (I - J^{+}J)z \tag{4}$$

where z is an arbitrary n-vector and $(I - J^{+}J)z$ represents the orthogonal projection of z onto the null space of J. Liégeois [10] used z to optimize a criterion function $g(\theta)$ subject to making the end effector follow a prescribed trajectory by setting $z = \alpha\nabla g(\theta)$. This null space term has also been used for several other objectives including those listed previously [7], [11], [14], [21].

This work will consider generalized inverse strategies to solve (2) which are of the form

$$\dot{\theta} = G\dot{x} \tag{5}$$

where G satisfies $JG = I$ for nonsingular configurations. The elements of G are functions of only the joint configuration. This strategy may be chosen to locally minimize a given criterion function such as a least-squares minimum norm criterion on the joint velocities as in the case of the pseudoinverse solution. Also popular in the robotics literature are weighted pseudoinverse solutions which locally minimize $\dot{\theta}^T Q \dot{\theta}$ for some positive definite weighting matrix Q such as the inertia matrix [20]. Due to the additional freedom afforded to kinematically redundant manipulators, control strategies such as (5) may not be repeatable in the sense that closed trajectories in the work space are not necessarily mapped to closed trajectories in the joint space so that for cyclic tasks the manipulator will not necessarily return to its starting configuration. Klein and Huang [9] give a proof of this for the pseudoinverse control of a three-link revolute manipulator. Such control strategies fail to give mappings which are one-to-one and onto.

Recently, there has been significant interest in this issue of repeatability [2], [4], [12], [13], [18], [19]. An elegant method for testing whether an inverse in the form of (5) is repeatable for simply connected, singularity-free subsets of the joint space was derived by Shamir and Yomdin [19]. This method, based on Frobenius's Theorem from differential geometry, consists of checking whether the Lie bracket of each pair of columns of G lies in the column space of G. This straightforward but tedious calculation can be used to determine if the manipulator is repeatable for particular regions of the joint space. It can also be used to determine candidates for what Shamir called "stable surfaces" which are surfaces on which the control is repeatable for nonsingular configurations.

Research has also been done on the construction of repeatable control strategies. Baker and Wampler have used topological methods to show that there may be inherent limitations on the regions of repeatability and that any repeatable control is equivalent to an inverse kinematic function over the specified domain [4]. Baillieul [2] devised a strategy which is repeatable in a simply connected, singularity-free subset of the joint space. This method, called the extended Jacobian, minimizes a criterion function of the joint variables for certain initial conditions and will be discussed in greater detail in the following section. Mussa-Ivaldi and Hogan [13] have also developed a class of repeatable inverses which use impedance control to devise strategies in the form of weighted pseudoinverses. Clearly, if one can identify an appropriate number of additional kinematic constraints that correspond to the desired use of the redundancy, augmenting the Jacobian with these equations is the method of choice for resolving the redundancy and automatically guaranteeing a repeatable solution [6], [17], [16].

The remainder of this paper is organized in the following manner: Section II describes a method for generating a generalized inverse G from the null space of G^T. This method characterizes a generalized inverse by the null space of its transpose. The relationship of this method to repeatability is discussed. Section III develops the mathematics required to define an appropriate class of augmenting vectors $\mathscr{V}$ which yield repeatable inverses. It is then shown how to choose the augmenting vector in $\mathscr{V}$ which minimizes its distance from a set of null vectors of G^T. Section IV uses a simple example to illustrate this technique with simulation results and a comparison to other repeatable control strategies appearing in Section V. In Section VI, an optimal repeatable inverse is calculated for a seven degree-of-freedom spatial manipulator in order to illustrate the generality of the technique. Finally, conclusions are presented in Section VII.

II. Augmented Jacobians

Generalized inverses such as those given in (5) can be generated by augmenting the Jacobian with the appropriate number of additional rows and performing a matrix inversion, provided of course that the augmented matrix is nonsingular. Suppose that J is augmented with additional rows represented here by the matrix N^T so that

$$J_N = \begin{bmatrix} J \\ \cdots \\ N^T \end{bmatrix}. \tag{6}$$

The inverse of J_N, if it exists, has the form

$$J_N^{-1} = \begin{bmatrix} G & \vdots & M \end{bmatrix} \tag{7}$$

where G is a generalized inverse of J and M is a maximal rank matrix whose column space is exactly the null space of J. Setting $z_N = N^T\dot{\theta}$ one obtains

$$\begin{bmatrix} \dot{x} \\ \cdots \\ z_N \end{bmatrix} = J_N \dot{\theta} \tag{8}$$

so that

$$\dot{\theta} = J_N^{-1} \begin{bmatrix} \dot{x} \\ \cdots \\ z_N \end{bmatrix} = G\dot{x} + Mz_N. \tag{9}$$

In order to obtain the control in (5) one merely sets $z_N = 0$. The converse is also true, i.e., that every generalized inverse G can be found by inverting an augmented Jacobian. In particular, this inverse is obtained by choosing N so that its column space is exactly the null space of G^T.

In this work, manipulators with a single degree of redundancy are considered so that N is given by the vector $\boldsymbol{v}$,

$$J_v = \begin{bmatrix} J \\ \cdots \\ v^T \end{bmatrix}, \tag{10}$$

and

$$J_v^{-1} = \left[G_v \quad \vdots \quad \frac{\boldsymbol{n}_J}{\boldsymbol{n}_J \cdot \boldsymbol{v}} \right] \tag{11}$$

where $\boldsymbol{n}_J$ is any null vector of J. If, for example, one chooses $\boldsymbol{v}$ to be proportional to $\boldsymbol{n}_J$ then G_v would be the pseudoinverse. One can consider the relationship of a generalized inverse and the set of its augmenting vectors as a one-to-one correspondence between the generalized inverses and an equivalence class on the augmenting vectors where only the direction of the augmenting vector is considered.

An example of an augmented Jacobian technique which guarantees repeatability in simply-connected, singularity-free subsets of the joint space is the extended Jacobian method discussed earlier [2]. This method utilizes the redundancy to optimize a criterion function $g(\theta)$ along with the primary constraint of following a specified end effector trajectory. Suppose the manipulator starts at an optimal configuration θ^* for a given end effector position and orientation. Baillieul proved that a necessary condition for being at a local extremum is that the gradient of $g(\theta)$ possess no component along the null space, i.e.,

$$\nabla g(\theta^*) \cdot \boldsymbol{n}_J(\theta^*) = 0. \tag{12}$$

Combining the end effector constraint and the optimization criteria results in the equation

$$\begin{bmatrix} f(\theta) \\ \cdots \\ \nabla g \cdot \boldsymbol{n}_J \end{bmatrix} = \begin{bmatrix} x \\ \cdots \\ 0 \end{bmatrix}. \tag{13}$$

Differentiating (13) results in

$$\begin{bmatrix} J \\ \cdots \\ (\nabla(\nabla g \cdot \boldsymbol{n}_J))^T \end{bmatrix} \dot{\theta} = \begin{bmatrix} \dot{x} \\ \cdots \\ 0 \end{bmatrix} \tag{14}$$

where the matrix on the left-hand side is defined as the extended Jacobian, denoted J_e [2]. If J_e is nonsingular then one obtains the joint velocities by simply multiplying (14) by J_e^{-1}. Clearly, J_e will be singular at kinematic singularities of the original robot which correspond to the singularities of J. However, J_e may also become singular when any of the additional rows added to the Jacobian are a linear combination of the rows of J. Mathematically, these singularities can be identified by evaluating the equation

$$\boldsymbol{n}_J \cdot \nabla(\nabla g \cdot \boldsymbol{n}_J) = 0. \tag{15}$$

These types of singularities, which are typical of augmented Jacobians, were noted by Baillieul for which he coined the term "algorithmic singularities" [2].

The inversion of J_v where v is a gradient will result in a repeatable inverse [17] and likewise essentially all repeatable inverses are determined by gradient functions [18]. The regions of repeatability are limited to simply connected, singularity-free subspaces. By augmenting the Jacobian with a gradient one is resolving the manipulator's redundancy by adding to the kinematic equation an additional function h where $\boldsymbol{v} = \nabla h$. By adding this additional function the manipulator acts "mathematically" like a nonredundant manipulator assuming that the rows of J and $\boldsymbol{v}$ are linearly independent. Later a set of allowable augmenting vectors which result in repeatable control strategies will be defined. The elements of this set will consist of gradient functions. It is important to note that this technique is distinct from the extended Jacobian technique since there may be no function g which describes the desired optimization criterion. The proposed technique is able to handle more general optimization criteria which are not restricted to be only functions of θ. In particular, one can consider the minimum joint velocity norm solution obtained using the pseudoinverse, which will be used as an illustrative example in the remainder of this work. The same technique can be used for any other desirable generalized inverse G by substituting the null vectors of G^T. It can even be used for time-varying G by including the variable time in the definition of the inner product.

III. A Class of Optimal Repeatable Control Strategies

The main idea of this work is to choose a repeatable inverse G_r whose associated null space is "close" to the associated null space of the desired inverse G_d. This will be done by selecting a gradient which approximates the null space of G_d^T on some desirable, nonsingular region Ω of the joint space. In order to pursue this goal as well as to define what is meant by "close," it will be necessary to cast the problem in terms of the Hilbert space $\mathscr{L}_2(\Omega)$, the space of Lebesgue measurable functions $\boldsymbol{u}: \Omega \to \mathbb{R}^n$ which satisfy $\int_\Omega \|\boldsymbol{u}\|_2^2 \, d\theta < \infty$. One who is not familiar with measure theory may consider everything to be continuous since ultimately, due to the limitations placed on the allowable augmenting vectors, the solutions will be continuous vector functions on Ω. The inner product $\langle \cdot,\cdot \rangle_\Omega$ of this space for the two vector functions $\boldsymbol{u}, \boldsymbol{v}$ is given by

$$\langle \boldsymbol{u},\boldsymbol{v} \rangle_\Omega = \int_\Omega \boldsymbol{u} \cdot \boldsymbol{v} \, d\theta \tag{16}$$

where $\boldsymbol{u} \cdot \boldsymbol{v}$ is the standard dot product and $\int_\Omega d\theta$ is the Lebesgue integral on $\Omega \subset \Theta$. The corresponding integral norm

$$\|\boldsymbol{u}\|_\Omega = \left[\int_\Omega \|\boldsymbol{u}\|_2^2 \, d\theta \right]^{\frac{1}{2}} \tag{17}$$

will be used as a measure of the distance between vector functions on Ω. Since $\mathscr{L}_2(\Omega)$ is a Hilbert space it follows that for any closed subspace $\mathscr{U}$ and any $\boldsymbol{w} \in \mathscr{L}_2(\Omega)$ there exists a unique $\boldsymbol{u} \in \mathscr{U}$ such that $\|\boldsymbol{u} - \boldsymbol{w}\|_\Omega$ is minimal.

While $\|\boldsymbol{u} - \boldsymbol{w}\|_\Omega$ gives a measure of the distance between two elements $\boldsymbol{u}$ and $\boldsymbol{w}$ in $\mathscr{L}_2(\Omega)$, it is also necessary to consider the measure of the distance between subsets of $\mathscr{L}_2(\Omega)$. The measure of the distance between two subsets F and G of $\mathscr{L}_2(\Omega)$ is defined to be $\operatorname{dist}(F,G) =$

$\inf\{\|u - v\|_\Omega | u \in F, v \in G\}$. In particular, this work is concerned with the distance between a normalized subset of the continuous null vectors of J and a space of allowable augmenting vectors $\mathscr{V}_a$. A desirable gradient v^* will have the property that it minimizes its distance to the subset of normalized null vectors. Clearly, for any vector function n the element in $\mathscr{V}_a$ which minimizes $\|v - n\|_\Omega$ is exactly the orthogonal projection of n onto $\mathscr{V}_a$.

A rigorous definition can now be made of an allowable space of augmenting vectors which will define the repeatable control strategies of interest. Consider the space $\mathscr{V} = \{\nabla g \in \mathscr{L}_2(\Omega) | g \in C^1(\Omega)\}$. An allowable space of augmenting vectors $\mathscr{V}_a$ is defined to be any closed linear subspace of $\mathscr{V}$ which has an orthonormal basis $\{v_i\}_{i \geq 1}$. A discussion of how to obtain such an orthonormal basis will be given later. The property that the subspace is closed is important since this guarantees that for any vector function u in $\mathscr{L}_2(\Omega)$ there is an element in the subspace $\mathscr{V}_a$ which is closest to u. An example of such a subspace is the span of any finite orthonormal subset of $\mathscr{V}$. With these restrictions on $\mathscr{V}_a$ the Projection Theorem guarantees that the element of $\mathscr{V}_a$ which is closest to some arbitrary vector function n in $\mathscr{L}_2(\Omega)$ is given by

$$v^*(n) = \sum_{i \geq 1} \langle n, v_i \rangle_\Omega v_i \tag{18}$$

which is simply the orthogonal projection of n onto $\mathscr{V}_a$.

In practice, to perform these calculations one is forced to consider a finite-dimensional subspace of $\mathscr{V}$. Let this subspace be denoted by $\mathscr{V}_N$ where N is the dimension and let $\{v_j\}_{j=1}^N$ be an orthonormal basis for $\mathscr{V}_N$. Now that an appropriate subspace has been defined, one can choose an augmenting vector from this set which minimizes its distance from $\mathscr{N}_0$, the set of continuous null vectors which are of unit length in the norm $\|\cdot\|_\Omega$. Note that any such null vector in $\mathscr{N}_0$ has the form $\alpha \hat{n}_J$ where $\|\hat{n}_J\|_2 = 1$, and α is in $\mathscr{A} = \{\alpha \in C(\Omega) | \int_\Omega \alpha^2\, d\theta = 1\}$ where $C(\Omega)$ represents the continuous real-valued functions on Ω. Thus the problem becomes that of finding the α^* in $\mathscr{A}$ and the v in $\mathscr{V}_N$ which minimizes $\|\alpha^* \hat{n}_J - v\|_\Omega^2$. This minimization will be done in three steps. First, the form of the α's which are closest to $\mathscr{V}_N$ will be derived. Then, the corresponding v in $\mathscr{V}_N$ for each of the candidate α's is calculated. Finally, the minimal pair is chosen from these candidates.

The n in $\mathscr{N}_0$ which is closest to a v in $\mathscr{V}_N$ is characterized in terms of its corresponding α by the following proposition.

Proposition 1: Let $v = \sum_{i=1}^N c_i v_i$ be a fixed vector function in $\mathscr{V}_N$ and suppose that $\sum_{i=1}^N c_i v_i \cdot \hat{n}_J \neq 0$. Suppose $\alpha^* = \arg\min_{\alpha \in \mathscr{A}} \|\alpha \hat{n}_J - \sum_{i=1}^N c_i v_i\|_\Omega^2$. Then there exists a constant K such that

$$\alpha^* = K \sum_{i=1}^N c_i v_i \cdot \hat{n}_J. \tag{19}$$

Proof: See Appendix A. Thus the candidate α's are of the form given in (19) so that it is only necessary to consider $\hat{\mathscr{A}}$, the set of functions in $\mathscr{A}$ which have this form.

For each $n \in \mathscr{N}_0$ the corresponding $v \in \mathscr{V}_N$ which is closest to n is the orthogonal projection of n onto $\mathscr{V}_N$. Let α be in $\hat{\mathscr{A}}$ and let $v(\alpha)$ denote the orthogonal projection of $\alpha \hat{n}_J$ onto $\mathscr{V}_N$. The problem now becomes to minimize $\|\alpha \hat{n}_J - v(\alpha)\|_\Omega$ over the scalar functions α in $\hat{\mathscr{A}}$. Since α is in $\hat{\mathscr{A}}$, there exist $b_1, \cdots, b_N$ such that

$$\alpha = \sum_{j=1}^N b_j v_j \cdot \hat{n}_J. \tag{20}$$

Let $a_i(\alpha)$ be the generalized Fourier coefficient of $\alpha \hat{n}_J$ corresponding to v_i. From (20) it follows that

$$a_i(\alpha) = \langle \alpha \hat{n}_J, v_i \rangle_\Omega = \sum_{j=1}^N b_j \int_\Omega (v_i \cdot \hat{n}_J)(v_j \cdot \hat{n}_J)\, d\theta. \tag{21}$$

In order to make the presentation clearer some vector notation is introduced. Let $a = [a_1(\alpha), \cdots, a_N(\alpha)]^T$ correspond to the generalized Fourier coefficients defined in (21), $b = [b_1, \cdots, b_N]$, and let the matrix M be the Gramian matrix defined by

$$M_{ij} = \int_\Omega (v_i \cdot \hat{n}_J)(v_j \cdot \hat{n}_J)\, d\theta. \tag{22}$$

Using this notation (21) becomes

$$a = Mb. \tag{23}$$

In order for $\|\alpha \hat{n}_J\|_\Omega = 1$ there is a restriction on b. Integrating the square of (20) yields

$$\int_\Omega \alpha^2\, d\theta = \sum_{i=1}^N \sum_{j=1}^N \int_\Omega (v_i \cdot \hat{n}_J)(v_j \cdot \hat{n}_J)\, d\theta\, b_i b_j, \tag{24}$$

which is equal to one, which in vector notation becomes

$$b^T M b = 1. \tag{25}$$

Now $\|\alpha \hat{n}_J - v(\alpha)\|_\Omega^2 = 1 - a^T a$. Thus, it is important to maximize $a^T a$ subject to (25). This maximum occurs when a and b are eigenvectors of M associated with its largest eigenvalue. Since M is a symmetric positive semidefinite matrix, a can be found from the singular value decomposition of M. The vector a would simply be $\sqrt{\sigma_1}\, u_1$ where σ_1 is the largest singular value and u_1 is its corresponding singular vector. It is this vector of generalized Fourier coefficients which minimizes the distance to $\mathscr{N}_0$. For the case when there are multiple maximum singular values, any linear combination of the corresponding singular vectors which has been normalized to a length of $\sqrt{\sigma_1}$ results in an optimal solution. Thus, when the optimal is nonunique the singular value decomposition of M gives a characterization for all of the optimal solutions.

As well as providing a tool for calculating the optimal solution for a given basis the Gramian formulation also provides a measure that one can use to compare any other augmenting vector. For an augmenting vector v the Gramian matrix with respect to the normalized vector function $\tilde{v} = v/\|v\|_\Omega$ is a scalar given by

$$m' = \int_\Omega (\hat{n}_J \cdot \tilde{v})(\hat{n}_J \cdot \tilde{v})\, d\theta = \frac{1}{\|v\|_\Omega^2} \int_\Omega (\hat{n}_J \cdot v)(\hat{n}_J \cdot v)\, d\theta. \tag{26}$$

If v is in the span of the basis $\{v_1, \cdots, v_N\}$ then the Gramian matrix M defined in (22) can be directly used to determine how close a match v is to the null space. The vector function v has the form $v = \Sigma_{i=1}^N c_i v_i$ for some set of real constant scalars $c_1, c_2, \cdots, c_N$. Representing v in the vector form $c = [c_1 \cdots c_N]^T$ one obtains that

$$m' = \frac{c^T M c}{c^T c}. \tag{27}$$

The closer m' is to one, the closer v is to approximating a null vector of the desired inverse.

In order to perform the above calculations one must determine an orthonormal basis for the allowable augmenting vectors. At first this may appear to be difficult since the elements must be gradients as well as orthonormal. Fortunately, there is an easy method for doing this. Consider a simply-connected region $\Omega = I_1 \times I_2 \times \cdots \times I_n$ where $I_i = [a_i, b_i]$ with $a_i < b_i$. The standard Fourier functions for the θ_i component on the interval I_i are given by

$$\left\{ \frac{1}{\sqrt{2}} K_i, K_i \sin \frac{2n\pi}{|I_i|}(\theta_i - c_i), K_i \cos \frac{2n\pi}{|I_i|}(\theta_i - c_i) \right\}_{n \geq 1} \tag{28}$$

$$J = \begin{bmatrix} -\sin\theta_1 - \sin\theta_{12} - \sin\theta_{123} & -\sin\theta_{12} - \sin\theta_{123} & -\sin\theta_{123} \\ \cos\theta_1 + \cos\theta_{12} + \cos\theta_{123} & \cos\theta_{12} + \cos\theta_{123} & \cos\theta_{123} \end{bmatrix} \tag{29}$$

where $|I_i| = b_i - a_i$, $c_i = (a_i + b_i)/2$ and $K_i = \sqrt{2/|I_i|}$. The Fourier functions on Ω, denoted here by ρ_j, are simply permutations of the products of the Fourier functions for each I_i described by the set given in (28). The set $\{\rho_j\}_{j \geq 1}$ forms a basis for the scalar functions on Ω. By taking the gradient of each ρ_j one can obtain a basis for a subset of gradients. It is important to note that this basis does not span the entire space of gradient functions. However, the set $\{\nabla\rho_j\}_{j \geq 1}$ does form an orthogonal basis for a proper subset of the gradients (see Appendix B), which is crucial for the success of this technique. An example of a set of gradients not obtained by differentiating the set $\{\rho_j\}_{j \geq 1}$ is the set of gradients represented by the standard basis $\{e_1, e_2, \cdots, e_n\}$ on $\mathbb{R}^n$. Since this set is orthogonal to the set $\{\nabla\rho_j\}_{j \geq 1}$, the two sets can be concatenated to obtain a larger orthogonal basis. Reducing this set to N terms and normalizing each element in the norm $\|\cdot\|_\Omega$ results in the space $\mathscr{V}_N = \mathrm{span}\{v_i\}_{i=1}^N$ where each v_i is in the form of a normalized $\nabla\rho_j$ or e_j. The space $\mathscr{V}_N$ forms a closed subspace of $\mathscr{L}_2(\Omega)$ where each member is a gradient function. Note that, in general, performing the gradient operation on an orthogonal basis other than (28) will not yield an orthogonal basis of gradients. For example, if one were to use orthogonal polynomials, one would not necessarily obtain an orthogonal set of gradients after differentiating.

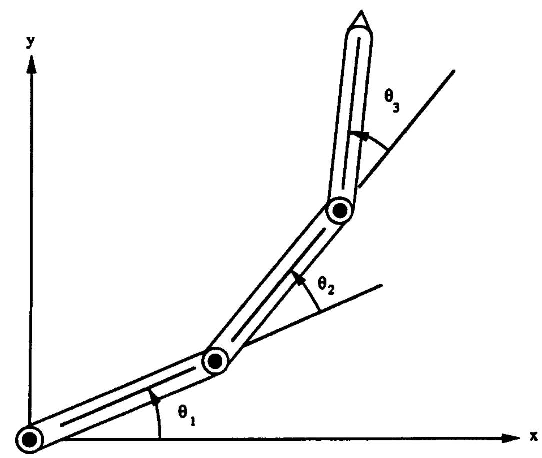

Fig. 1. Geometry of a planar three degree-of-freedom manipulator with revolute joints and unit link lengths.

IV. A Simple Example

In order to illustrate the technique described in the previous section consider the simple three-link planar manipulator shown in Fig. 1 which has links of unit length. The Jacobian for this manipulator is given by (29) where $\theta_{ij} = \theta_i + \theta_j$. For a simply-connected, singularity-free subset of the joint space the unit null vector $\hat{n}_J$ for this manipulator can be continuously and uniquely defined up to a multiple of -1. In particular it can be obtained by normalizing the cross product of the two rows of the Jacobian:

$$\hat{n}_J = \frac{1}{\Delta} \begin{bmatrix} \sin\theta_3 \\ -\sin\theta_3 - \sin\theta_{23} \\ \sin\theta_2 + \sin\theta_{23} \end{bmatrix} \tag{30}$$

where

$$\Delta = \sqrt{\sin^2\theta_3 + (\sin\theta_3 + \sin\theta_{23})^2 + (\sin\theta_2 + \sin\theta_{23})^2}.$$

For this example the desired optimization criterion will be to minimize the norm of the joint angle velocities. The exact solution for this criterion is given by the pseudoinverse of the Jacobian; however, it is well-known that the pseudoinverse is not repeatable. Since the class of augmenting vectors associated with the pseudoinverse is characterized by the null vectors of the Jacobian, the task at hand is to find a gradient augmenting vector that most closely matches a null vector of the Jacobian in a simply connected, singularity-free region $\Omega = I_1 \times I_2 \times I_3$ where $I_i = [a_i, b_i]$ with $a_i < b_i$ for $i = 1,2,3$. The boundaries of this region can be chosen based on the particular physical constraints of the manipulator or the requirements of the task being performed. For this example, Ω will be taken to be $[\pi/4, 3\pi/4]^3$. Thus, (28) becomes

$$\left\{\sqrt{\frac{2}{\pi}}, \frac{2}{\sqrt{\pi}} \sin 4n\theta_i, \frac{2}{\sqrt{\pi}} \cos 4n\theta_i\right\}_{n \geq 1}. \tag{31}$$

For the purposes of illustration, the following orthonormal set of nine vector functions will be used

$$\{K_1 e_i, K_2 \cos 4\theta_i e_i, K_2 \sin 4\theta_i e_i\}_{i=1,2,3} \tag{32}$$

where $K_1 = (2/\pi)^{3/2}, K_2 = 4/\pi^{3/2}$, and where once again e_i represents the standard basis for $\mathbb{R}^3$. Let $\mathscr{V}_9$ denote the span of the above set. It can be easily verified that this is an orthonormal subset of $\mathscr{V}$.

The fact that $\mathscr{V}_9$ is closed guarantees that there is an element in $\mathscr{V}_9$ which is closest to some n_J in $\mathscr{N}_0$. Thus, from the Projection Theorem it follows that for each $n_J \in \mathscr{N}_0$ the unique $v^* \in \mathscr{V}_9$ which minimizes its distance from n_J is given by

$$v^* = \sum_{j=1}^{9} \langle n_J, v_j \rangle_\Omega v_j \tag{33}$$

where $v_j = \nabla\rho_j / \|\nabla\rho_j\|_\Omega$. The Gramian matrix corresponding to $\mathscr{V}_9$ is calculated using (22) and is given below:

$$M = \begin{bmatrix} 0.4275 & -0.2557 & 0.2579 & 0.0000 & -0.0124 & 0.0160 & 0.0000 & 0.0200 & -0.0141 \\ -0.2557 & 0.2844 & -0.2813 & 0.0000 & -0.0073 & -0.0040 & 0.0000 & -0.0753 & 0.0773 \\ 0.2579 & -0.2813 & 0.2881 & 0.0000 & -0.0158 & -0.0211 & 0.0000 & 0.0791 & -0.0733 \\ 0.0000 & 0.0000 & 0.0000 & 0.4275 & 0.0000 & 0.0000 & 0.0000 & 0.0000 & 0.0000 \\ -0.0124 & -0.0073 & -0.0158 & 0.0000 & 0.2849 & -0.0210 & 0.0000 & 0.0263 & 0.0107 \\ 0.0160 & -0.0040 & -0.0211 & 0.0000 & -0.0210 & 0.2915 & 0.0000 & 0.0093 & 0.0258 \\ 0.0000 & 0.0000 & 0.0000 & 0.0000 & 0.0000 & 0.0000 & 0.4275 & 0.0000 & 0.0000 \\ 0.0200 & -0.0753 & 0.0791 & 0.0000 & 0.0263 & 0.0093 & 0.0000 & 0.2839 & 0.0287 \\ -0.0141 & 0.0773 & -0.0733 & 0.0000 & 0.0107 & 0.0258 & 0.0000 & 0.0287 & 0.2847 \end{bmatrix}. \tag{34}$$

Since M is symmetric it can be decomposed in the form USU^T where U is a unitary matrix and S is a diagonal matrix. For this case

$$U = \begin{bmatrix} -0.6067 & 0.0000 & 0.0000 & 0.0723 & -0.2126 & -0.4311 & -0.0112 & 0.6288 & 0.0076 \\ 0.5407 & 0.0000 & 0.0000 & 0.0061 & -0.0601 & -0.0900 & 0.0603 & 0.4485 & -0.7008 \\ -0.5449 & 0.0000 & 0.0000 & -0.0429 & 0.0624 & 0.0868 & 0.0710 & -0.4304 & -0.7067 \\ 0.0000 & 0.9998 & 0.0220 & 0.0000 & 0.0000 & 0.0000 & 0.0000 & 0.0000 & 0.0000 \\ 0.0159 & 0.0000 & 0.0000 & 0.2368 & 0.6577 & -0.3065 & -0.6425 & -0.0102 & -0.0646 \\ 0.0026 & 0.0000 & 0.0000 & 0.4532 & -0.6007 & 0.2961 & -0.5813 & -0.0592 & -0.0684 \\ 0.0000 & -0.0220 & 0.9998 & 0.0000 & 0.0000 & 0.0000 & 0.0000 & 0.0000 & 0.0000 \\ -0.1495 & 0.0000 & 0.0000 & 0.5425 & 0.3777 & 0.5873 & 0.2957 & 0.3288 & 0.0173 \\ 0.1412 & 0.0000 & 0.0000 & 0.6612 & -0.1058 & -0.5215 & 0.3912 & -0.3263 & 0.0156 \end{bmatrix} \tag{35}$$

and

$$S = \mathrm{diag}(0.8956, 0.4275, 0.4275, 0.3337, 0.3206, 0.2580, 0.2495, 0.0851, 0.0025). \tag{36}$$

The largest eigenvalue of M is 0.8956 with the corresponding unit length eigenvector

$$u_1 = \begin{bmatrix} -0.6067 \\ 0.5407 \\ -0.5449 \\ 0 \\ 0.0159 \\ 0.0026 \\ 0 \\ -0.1495 \\ 0.1412 \end{bmatrix}^T. \tag{37}$$

Thus, the vector function in $\mathscr{V}_9$ which has minimum distance from $\mathscr{N}_0$ is given by

$$\sqrt{0.8956}\left(\frac{2\sqrt{2}}{\pi^{3/2}}\right) \cdot \begin{bmatrix} -0.6067 \\ 0.5407 + 0.0159\sqrt{2}\cos(4\theta_2) - 0.1495\sqrt{2}\sin(4\theta_2) \\ -0.5449 + 0.0026\sqrt{2}\cos(4\theta_3) - 0.1412\sqrt{2}\sin(4\theta_3) \end{bmatrix}. \tag{38}$$

V. Simulation Results

In order to compare the performance of the repeatable inverse obtained using the technique described above with that of the desired nonrepeatable inverse (in this case, the pseudoinverse) a number of simulations were performed. A representative end effector trajectory for the planar manipulator used in the example above is given in Fig. 2. This trajectory was selected so that the starting point is at the image of the center of the desired operating range Ω and so that it is far from any singularities. The initial configuration for all simulations is taken as $\theta(0) = [\pi/2 \;\; \pi/2 \;\; \pi/2]^T$ which is, once again, the center of the desired

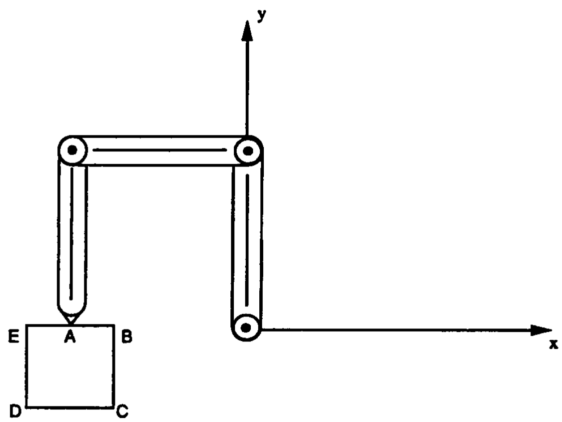

Fig. 2. The initial manipulator configuration and the desired end effector trajectory used in the simulations.

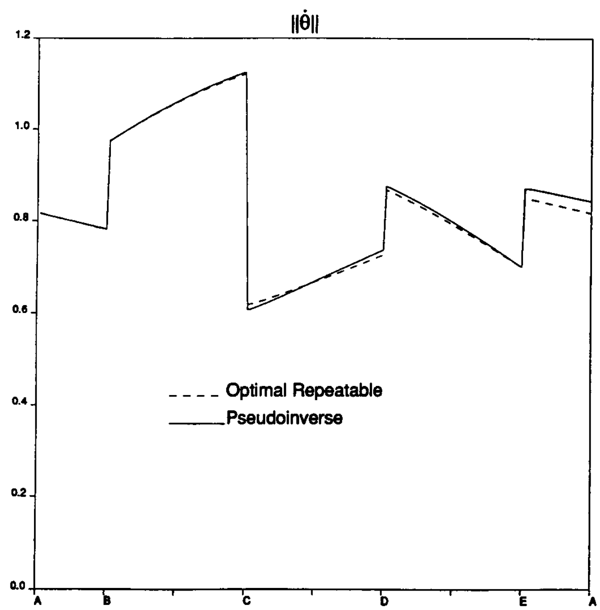

Fig. 3. A comparison of the norm of the joint angle velocity required to follow the trajectory given in Fig. 2 using the pseudoinverse and the optimal repeatable inverse obtained when using the basis given by $\mathscr{V}_9$.

operating range Ω. Fig. 3 presents a comparison of the norm of the joint angle velocity required for the end effector to traverse the trajectory shown in Fig. 2 for both the pseudoinverse and the repeatable inverse obtained by using the augmenting vector given by (38). Note that the norm of the joint angle velocity for the pseudoinverse is not the same at the start and at the end of the trajectory, illustrating that it is indeed not repeatable. By comparing the difference between the norms of the repeatable solution and the pseudoinverse solution one can qualitatively claim that the designed repeatable solution is a reasonable approximation to the desired performance of the pseudoinverse. It is also not surprising that the joint velocity norm for the repeatable inverse is in some cases smaller than that of the pseudoinverse solution since the pseudoinverse is only a local optimum and the manipulator configurations resulting from the two controls are different. One can quantitatively assess the performance difference between the two solutions over the entire set of possible end effector trajectories and initial conditions by examining m' which provides a measure of the accuracy to which the desired null vector is matched. By evaluating (27) using the coefficients from (38) one obtains $m' = 0.8956$ which is of course identical to σ_1 of M. Since an exact match of the desired null vector is by definition given by $m' = 1$ one can justifiably argue that the designed repeatable inverse is a good approximation to the desired pseudoinverse. Unfortunately, it is typically not possible to analytically determine the maximum value of m' for the set of all repeatable inverses so that one should perform the optimization over various different orthonormal bases in order to determine if the resulting performance difference is due to the inherent penalty of requiring repeatability.

In order to further illustrate some of the properties of the repeatable inverses obtained using the technique shown above, Fig. 4 presents a plot of the norm of the difference between the joint velocity obtained by using a repeatable inverse as opposed to the pseudoinverse. Three different repeatable inverses resulting from three different augmenting vectors are compared where each is evaluated from the configuration that would result from using pseudoinverse control. The first augmenting vector is that given by (38) which is the optimal when using the basis given by $\mathscr{V}_9$. The second augmenting vector is given by

$$v = \begin{bmatrix} -0.6367 \\ 0.5434 \\ -0.5472 \end{bmatrix}. \tag{39}$$

which is the optimal when using the smaller orthogonal basis $\mathscr{V}_3$ which is composed of only the three standard basis vectors $\{e_1, e_2, e_3\}$. Note that to calculate the optimal augmenting vector for this basis one must redo the matrix decomposition on the upper left-hand three by three partition of M given in (34) since the optimal coefficients for these terms will in general be different from those obtained when using additional terms. It is also instructive to notice that the optimal augmenting vector given by (39) is very close to the vector that would be obtained by evaluating the desired null vector given by (30) at the center of the region of interest Ω. The third augmenting vector used in the comparison is given by

$$v = \begin{bmatrix} 0 \\ 1 \\ 0 \end{bmatrix} \tag{40}$$

which is selected on the basis of its simplicity as well as the fact that it effectively results in an isotropic two degree-of-freedom manipulator configuration at the cen-

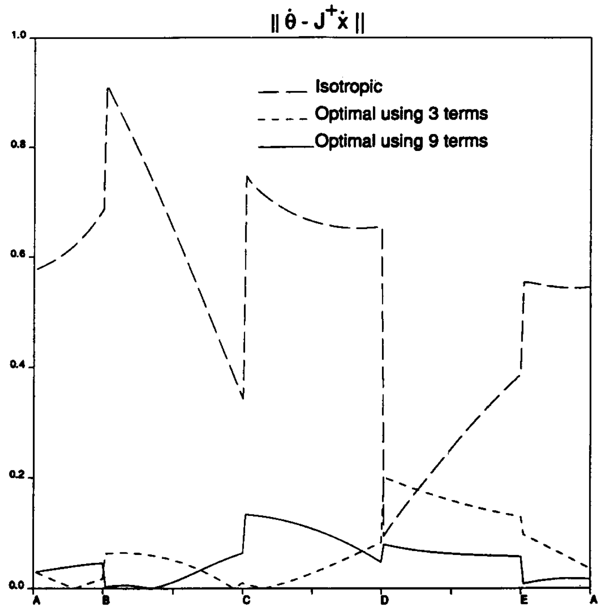

Fig. 4. A comparison of the norm of the difference between a repeatable inverse and the pseudoinverse for three different augmenting vectors. All controls are calculated locally from the configuration that results from using the pseudoinverse.

ter of Ω. By comparing the performance of these three repeatable inverses, it is clear that both of the inverses that are calculated using the technique illustrated here perform significantly better than the inverse resulting from the rather unsophisticated choice of the augmenting vector given by (40). The performance of the optimal solutions using the bases $\mathscr{V}_3$ and $\mathscr{V}_9$ are comparable with neither being obviously superior. A quantitative comparison of their performance is obtained by noting that the value of m' for the $\mathscr{V}_3$ inverse is 0.8674 which is marginally worse than the 0.8956 value obtained for the $\mathscr{V}_9$ inverse as would be expected. Both of these values are far superior to the value of $m' = 0.2844$ for the inverse using the simple augmenting vector given by (40). Thus, even when dealing with a very small number of functions in the orthonormal basis, one can still obtain a very good approximation of the null vector of the desired inverse.

VI. A Spatial Seven Degree-of-Freedom Example

In order to illustrate the generality of the technique presented here, this section discusses the calculation of an optimal repeatable inverse for a fully general spatial manipulator. The manipulator under consideration is the seven degree-of-freedom manipulator discussed in [15] which is of a typical anthropomorphic design with a three degree-of-freedom shoulder, a one degree-of-freedom elbow, and a three degree-of-freedom wrist. While the calculations are more computationally expensive in this case as opposed to the planar case, the procedure is identical. In particular, one first selects a region of interest Ω in the joint space over which the repeatable inverse is to approximate the desired inverse. Since this manipulator has seven degrees-of-freedom the region of interest is given by $\Omega = I_1 \times I_2 \times \cdots \times I_7$ where for the purpose of illustration the intervals are selected as $I_5 = [-\pi/4, \pi/4]$ with all other intervals $I_i = [\pi/4, 3\pi/4]$.

The next step is the selection of a finite set of N orthogonal basis functions which will be used to approximate the null vector of the desired inverse. As pointed out in Section III an orthogonal basis for the continuous real-valued functions can be obtained as the product of the Fourier functions given in (28). Performing the gradient operation and normalizing with respect to $\|\cdot\|_\Omega$ yields an orthonormal basis for a subset of gradients. By properly scaling the elements of the standard basis $\{\boldsymbol{e}_1, \boldsymbol{e}_2, \cdots, \boldsymbol{e}_n\}$ one can add additional elements to make a larger basis of orthonormal gradients. The number of basis functions N that one selects depends on the desired accuracy and the amount of computational expense that one can afford. In practice, the terms from the standard basis tend to be the most significant since they correspond to the "DC" terms of the generalized Fourier series. Thus, for this example the orthogonal basis for the allowable set of augmenting vectors will be chosen as the standard basis for $\mathbb{R}^7$ so that $N = 7$.

After a finite set of orthonormal gradient functions has been chosen one must now calculate the N by N Gramian matrix M as given by (22). Each element of M is determined by an n-dimensional integration over the region Ω. This calculation requires the null vector of the Jacobian which for this example is given by [15]

$$\boldsymbol{n}_J = \begin{bmatrix} \cos\theta_3 \sin\theta_4 \sin\theta_6 h \\ -\sin\theta_2 \sin\theta_3 \sin\theta_4 \sin\theta_6 h \\ -(\sin\theta_2 g + \sin\theta_2 \cos\theta_4 h + \cos\theta_2 \cos\theta_3 \sin\theta_4 h)\sin\theta_6 \\ 0 \\ \sin\theta_2 \cos\theta_4 \sin\theta_6 g + \sin\theta_2 \sin\theta_4 \cos\theta_5 \cos\theta_6 g + \sin\theta_2 \sin\theta_6 h \\ \sin\theta_2 \sin\theta_4 \sin\theta_5 \sin\theta_6 g \\ -\sin\theta_2 \sin\theta_4 \cos\theta_5 g \end{bmatrix} \tag{41}$$

where the link lengths g and h will be taken to be 1 meter. It is important to point out that while such an analytical expression for the null vector is desirable, it is not required. One can always numerically determine the null vector for a given configuration when calculating (22). For this example these computations resulted in

$$M = \begin{bmatrix} 0.0515 & 0.0000 & 0.0000 & 0.0000 & 0.0000 & 0.0000 & 0.0000 \\ 0.0000 & 0.1861 & 0.1845 & 0.0000 & -0.1728 & 0.0000 & 0.2046 \\ 0.0000 & 0.1845 & 0.2391 & 0.0000 & -0.2165 & 0.0000 & 0.2049 \\ 0.0000 & 0.0000 & 0.0000 & 0.0000 & 0.0000 & 0.0000 & 0.0000 \\ 0.0000 & -0.1728 & -0.2165 & 0.0000 & 0.2501 & 0.0000 & -0.1903 \\ 0.0000 & 0.0000 & 0.0000 & 0.0000 & 0.0000 & 0.0417 & 0.0000 \\ 0.0000 & 0.2046 & 0.2049 & 0.0000 & -0.1903 & 0.0000 & 0.2316 \end{bmatrix}. \tag{42}$$

Note that the fourth row and column of M are identically zero due to the fact that the null vector for this manipulator never has any component of the fourth joint. Identifying such properties of the null vector can allow one to immediately discount certain basis functions, such as $\boldsymbol{e}_4$ in this case, since they will not appear in the optimal augmenting vector.

Once the symmetric matrix M has been calculated, its singular value decomposition $M = USU^T$ is used to find the optimal coefficients for the basis of augmenting vectors. The singular value decomposition of (42) is given by

$$U = \begin{bmatrix} 0.000 & 0.000 & 1.000 & 0.000 & 0.000 & 0.000 & 0.000 \\ -0.458 & 0.439 & 0.000 & 0.000 & -0.176 & -0.753 & 0.000 \\ -0.520 & -0.218 & 0.000 & 0.000 & 0.826 & -0.004 & 0.000 \\ 0.000 & 0.000 & 0.000 & 0.000 & 0.000 & 0.000 & 1.000 \\ 0.511 & 0.696 & 0.000 & 0.000 & 0.504 & -0.023 & 0.000 \\ 0.000 & 0.000 & 0.000 & -1.000 & 0.000 & 0.000 & 0.000 \\ -0.509 & 0.525 & 0.000 & 0.000 & -0.179 & 0.658 & 0.000 \end{bmatrix} \tag{43}$$

and

$$S = \operatorname{diag}(0.8154, 0.0653, 0.0515, 0.0417, 0.0232, 0.0029, 0.0000). \tag{44}$$

The optimal augmenting vector is simply a normalized version of the singular vector associated with the largest singular value of M. Thus, the optimal repeatable inverse would be obtained by using

$$\sqrt{0.8154}\,[0 \;\; -0.458 \;\; -0.520 \;\; 0 \;\; 0.511 \;\; 0 \;\; -0.509] \tag{45}$$

as the augmenting row of the Jacobian. Note that once again the vector given by (45) is very close to what one obtains from evaluating (41) at the center of Ω. Further evidence that the resulting repeatable inverse represents a good approximation of the desired performance of the pseudoinverse over the entire range of Ω is given by noting that $m' = 0.8154$.

VII. Conclusion

The contribution of this work is a technique for generating a repeatable generalized inverse which is close to some arbitrary generalized inverse that possesses desirable properties. This technique relies on using orthonormal basis functions to describe a set of possible gradient functions. While this is in general a formidable task, it was shown that for this particular application, simple trigonometric functions are an ideal choice. It was also shown that the optimal coefficients for these basis functions can be easily determined by calculating the singular vector associated with the maximum singular value of the Gramian matrix. Examples were presented which illustrate that the resulting approximations to the desired inverse can be quite good, even when using a small number of basis functions.

Appendix A

Proposition 1: Let $\boldsymbol{v} = \sum_{i=1}^{N} c_i \boldsymbol{v}_i$ be a fixed vector function in $\mathscr{V}_N$ and suppose that $\sum_{i=1}^{N} c_i \boldsymbol{v}_i \cdot \hat{\boldsymbol{n}}_J \neq 0$. Let $\alpha^* = \arg\min_{\alpha \in \mathscr{A}} \| \alpha \hat{\boldsymbol{n}}_J - \sum_{i=1}^{N} c_i \boldsymbol{v}_i \|_\Omega^2$. Then there exists a constant K such that

$$\alpha^* = K \sum_{i=1}^{N} c_i \boldsymbol{v}_i \cdot \hat{\boldsymbol{n}}_J. \tag{A1}$$

Proof: The function α^* solves the following problem:

$$\text{Minimize} \int_\Omega \left\| \alpha \hat{\boldsymbol{n}}_J - \sum_{i=1}^{N} c_i \boldsymbol{v}_i \right\|_2^2 d\theta \tag{A2}$$

$$\text{Subject to} \int_\Omega \alpha^2 \, d\theta = 1. \tag{A3}$$

The Euler–Lagrange equation must be satisfied in order for a minimum to occur. This equation is given by

$$\frac{\partial}{\partial \alpha} \left\| \alpha \hat{\boldsymbol{n}}_J - \sum_{i=1}^{N} c_i \boldsymbol{v}_i \right\|_2^2 + \lambda \frac{\partial}{\partial \alpha} \alpha^2 = 0 \tag{A4}$$

which becomes

$$2\alpha - 2 \sum_{i=1}^{N} c_i \boldsymbol{v}_i \cdot \hat{\boldsymbol{n}}_J + 2\lambda\alpha = 0. \tag{A5}$$

Separating terms results in

$$(1+\lambda)\alpha = \sum_{i=1}^{N} c_i \boldsymbol{v}_i \cdot \hat{\boldsymbol{n}}_J. \tag{A6}$$

Since $\sum_{i=1}^{N} c_i \boldsymbol{v}_i \cdot \hat{\boldsymbol{n}}_j \neq 0$, one obtains

$$\alpha = \frac{1}{1+\lambda}\sum_{i=1}^{N} c_i \boldsymbol{v}_i \cdot \hat{\boldsymbol{n}}_J. \tag{A7}$$

By setting $K = (1/1+\lambda)$, the lemma is proved. Note that K can be calculated from the fact that α is of unit length in the norm $\|\cdot\|_\Omega$. ■

Appendix B

Proposition 2: $\{\nabla\rho_j / \|\nabla\rho_j\|_\Omega\}_{j=1}^{N}$ is an orthonormal set.

Proof: In order to prove the proposition it suffices to show that any two distinct elements of the set are orthogonal. Let $j \neq k$ so that $\rho_j \neq \rho_k$. Both have the form of the product of trigonometric functions

$$\rho_j = R_{1m_1}(\theta_1)R_{2m_2}(\theta_2)\cdots R_{nm_n}(\theta_n) \tag{B1}$$

$$\rho_k = T_{1p_1}(\theta_1)T_{2p_2}(\theta_2)\cdots T_{np_n}(\theta_n) \tag{B2}$$

where R_{in} and T_{in} are Fourier functions on I_i of the form (28). The gradients are

$$\nabla\rho_j = \begin{bmatrix} R'_{1m_1}(\theta_1)R_{2m_2}(\theta_2)\cdots R_{nm_n}(\theta_n) \\ R_{1m_1}(\theta_1)R'_{2m_2}(\theta_2)\cdots R_{nm_n}(\theta_n) \\ \vdots \\ R_{1m_1}(\theta_1)R_{2m_2}(\theta_2)\cdots R'_{nm_n}(\theta_n) \end{bmatrix} \tag{B3}$$

and

$$\nabla\rho_k = \begin{bmatrix} T'_{1p_1}(\theta_1)T_{2p_2}(\theta_2)\cdots T_{np_n}(\theta_n) \\ T_{1p_1}(\theta_1)T'_{2p_2}(\theta_2)\cdots T_{np_n}(\theta_n) \\ \vdots \\ T_{1p_1}(\theta_1)T_{2p_2}(\theta_2)\cdots T'_{np_n}(\theta_n) \end{bmatrix} \tag{B4}$$

where R'_{im_i} and T'_{ip_i} represent the derivative with respect to θ_i of R_{im_i} and T_{ip_i}, respectively. The inner product of $\nabla\rho_j$ and $\nabla\rho_k$ is

$$\begin{aligned} \int_\Omega \nabla\rho_j \cdot \nabla\rho_k \, d\theta &= \int_\Omega \sum_{i=1}^{n} \Big(R'_{im_i}\prod_{l\neq i} R_{lm_l}\Big)\Big(T'_{ip_i}\prod_{l\neq i} T_{lp_l}\Big)\, d\theta \\ &= \sum_{i=1}^{n}\int_\Omega R'_{im_i}T'_{ip_i}\prod_{l\neq i} R_{lm_l}T_{lp_l}\, d\theta \\ &= \sum_{i=1}^{n}\int_{I_i} R'_{im_i}T'_{ip_i}\, d\theta_i \prod_{l\neq i}\int_{I_l} R_{lm_l}T_{lp_l}\, d\theta_l. \end{aligned} \tag{B5}$$

Since $\rho_j \neq \rho_k$ there is an i such that $R_{im_i} \neq T_{ip_i}$. Then R_{im_i} and T_{ip_i} are orthogonal and since both are of the form (28), R'_{im_i} and T'_{ip_i} are also orthogonal. It thus follows that

$$\int_\Omega \nabla\rho_i \cdot \nabla\rho_j \, d\theta = 0. \tag{B6}$$

■

References

[1] J. Baillieul, J. Hollerbach, and R. Brockett, "Programming and control of kinematically redundant manipulators," in *Proc. IEEE Conf. Decision Contr.*, Las Vegas, NV, Dec. 12–14, 1984, pp. 768–774.

[2] J. Baillieul, "Kinematic programming alternatives for redundant manipulators," in *Proc. IEEE Conf. Robotics Automat.*, St. Louis, MO, Mar. 1985, pp. 722–728.

[3] ——, "Avoiding obstacles and resolving redundancy," in *Proc. IEEE Conf. Robotics Automat.*, San Francisco, CA, Apr. 1986, pp. 1698–1703.

[4] D. R. Baker and C. W. Wampler II, "On the inverse kinematics of redundant manipulators," *Int. J. Robotics Res.*, vol. 7, no. 2, pp. 3–21, Mar.–Apr. 1988.

[5] R. Dubey and J. Y. S. Luh, "Redundant robot control for higher flexibility," in *Proc. IEEE Conf. Robotics Automat.*, Raleigh, NC, Mar.-Apr. 1987, pp. 1066–1072.

[6] O. Egeland, "Task-space tracking with redundant manipulators," *IEEE J. Robotics Automat.*, vol. RA-3, no. 5, pp. 471–475, Oct. 1987.

[7] J. M. Hollerbach and K. C. Suh, "Redundancy resolution of manipulators through torque optimization," *IEEE J. Robotics Automat.*, vol. RA-3, no. 4, pp. 308–316, Aug. 1987.

[8] C. A. Klein and B. E. Blaho, "Dexterity measures for the design and control of kinematically redundant manipulators," *Int. J. Robotics Res.*, vol. 6, no. 2, pp. 72–83, Summer 1987.

[9] C. A. Klein and C. H. Huang, "Review of pseudoinverse control for use with kinematically redundant manipulators," *IEEE Trans. Syst., Man, Cybern.*, vol. SMC-13, no. 3, pp. 245–250, Mar.-Apr. 1983.

[10] A. Liégeois, "Automatic supervisory control of the configuration and behavior of multibody mechanisms," *IEEE Trans. Syst., Man, Cybern.*, vol. SMC-12, no. 12, pp. 868–871, Dec. 1977.

[11] A. A. Maciejewski and C. A. Klein, "Obstacle avoidance for kinematically redundant manipulators in dynamically varying environments, " *Int. J. Robotics Res.*, vol. 4, no. 3, pp. 109–117, Fall 1985.

[12] A. A. Maciejewski and R. G. Roberts, "Utilizing kinematic redundancy in robotic systems: Practical implementations and fundamental limitations," in *Proc. Amer. Contr. Conf.*, San Diego, CA, May 23–25, 1990, pp. 209–214.

[13] F. A. Mussa-Ivaldi and N. Hogan, "Solving kinematic redundancy with impedance control: A class of integrable pseudoinverses," in *Proc. IEEE Conf. Robotics Automat.*, Scottsdale, AZ, 1989, pp. 283–288.

[14] Y. Nakamura, H. Hanafusa, and T. Yoshikawa, "Task-priority based redundancy control of robot manipulators," *Int. J. Robotics Res.*, vol. 6, no. 2, pp. 3–15, Summer 1987.

[15] R. P. Podhorodeski, A. A. Goldenberg, and R. G. Fenton, "Resolving redundant manipulator joint rates and identifying special arm configurations using Jacobian null-space bases," *IEEE Trans. Robotics Automat.*, vol. 7, no. 5, pp. 607–618, Oct. 1991.

[16] L. Sciavicco and B. Siciliano, "A solution algorithm to the inverse kinematic problem for redundant manipulators," *IEEE J. Robotics Automat.*, vol. 4, no. 4, pp. 403–410, Aug. 1988.

[17] H. Seraji, "Configuration control of redundant manipulators: Theory and implementation," *IEEE Trans. Robotics Automat.*, vol. 5, no. 4, pp. 472–490, Aug. 1991.

[18] T. Shamir, "Remarks on some dynamical problems of controlling redundant manipulators," *IEEE Trans. Automat. Contr.*, vol. 35, no. 3, pp. 341–344, Mar. 1990.

[19] T. Shamir and Y. Yomdin, "Repeatability of redundant manipulators: Mathematical solution of the problem," *IEEE Trans. Automat. Contr.*, vol. 33, no. 11, pp. 1004–1009, Nov. 1988.

[20] D. E. Whitney, "Resolved motion rate control of manipulators and human prostheses," *IEEE Trans. Man-Machine Syst.*, vol. MMS-10, pp. 47–53, June 1969.

[21] T. Yoshikawa, "Analysis and control of robot manipulators with redundancy," in *Robotics Research: The First International Symposium*, M. Brady and R. Paul, Eds., pp. 735–747. MIT Press, 1984.

[22] ——, "Manipulability of robotic mechanisms," *Int. J. Robotics Res.*, vol. 4, no. 2, pp. 3–9, Summer 1985.

[23] ——, "Dynamic manipulability of robot manipulators," *J. Robotic Syst.*, vol. 2, no. 1, pp. 113–124, 1985.

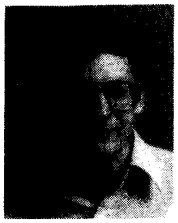

Rodney G. Roberts received the B.S. degrees in electrical engineering and mathematics from the Rose–Hulman Institute of Technology, Terre Haute, IN, in 1987 and the M.S.E.E. and Ph.D. degrees from Purdue University, West Lafayette, IN, in 1988 and 1992, respectively.

He is currently a National Research Council Fellow at Wright-Patterson Air Force Base. His research interest is in the motion control of robotic manipulators.

Anthony A. Maciejewski received the B.S.E.E., M.S., and Ph.D. degrees in electrical engineering from The Ohio State University, Columbus, in 1982, 1984, and 1987 respectively.

Since 1988 he has been an Assistant Professor with the School of Electrical Engineering at Purdue University, West Lafayette, IN. His primary research interests center on the simulation and control of kinematically redundant systems.